energies

MDPI

Perspective

Measurement and Modeling of Magnetic Materials under 3D Vectorial Magnetization for Electrical Machine Design and Analysis

Youguang Guo [1,*], Lin Liu [1,*], Xin Ba [1,*], Haiyan Lu [1], Gang Lei [1], Wenliang Yin [2] and Jianguo Zhu [2]

[1] Faculty of Engineering and Information Technology, University of Technology Sydney, Sydney, NSW 2007, Australia
[2] School of Electrical and Information Engineering, The University of Sydney, Sydney, NSW 2006, Australia
* Correspondence: youguang.guo-1@uts.edu.au (Y.G.); lin.liu@student.uts.edu.au (L.L.); xin.ba@student.uts.edu.au (X.B.); Tel.: +61-2-9514-2650 (Y.G.)

Abstract: The magnetic properties of magnetic cores are essential for the design of electrical machines, and consequently appropriate mathematical modeling is needed. Usually, the design and analysis of electrical machines consider only the one-dimensional (1D) magnetic properties of core materials, i.e., the relationship of magnetic flux density (B) versus magnetic field strength (H), and their associated power loss under 1D magnetization, in which the B and H are constrained in the same orientation. Some studies have also been performed with the two-dimensional (2D) magnetizations in which the B and H are vectorial, rotating on a plane, and they may not be in the same direction. It has been discovered that the 2D rotational property is very different from its 1D alternating counterpart. However, the magnetic fields in an electrical machine, in particular claw pole and transverse flux machines, are naturally three-dimensional (3D), and the B and H vectors are rotational and may not lie on the same plane. It can be expected that the 3D vectorial property might be different from its 2D or 1D counterpart, and hence it should be investigated for the interests of both academic research and engineering application. This paper targets at a general summary about the magnetic material characterization with 3D vectorial magnetization, and their application prospect in electrical machine design and analysis.

Keywords: magnetic material; magnetic property measurement; magnetic property modeling; three-dimensional (3D) vectorial magnetization; electrical machine

Citation: Guo, Y.; Liu, L.; Ba, X.; Lu, H.; Lei, G.; Yin, W.; Zhu, J. Measurement and Modeling of Magnetic Materials under 3D Vectorial Magnetization for Electrical Machine Design and Analysis. *Energies* **2023**, *16*, 417. https://doi.org/10.3390/en16010417

Academic Editor: Songling Huang

Received: 8 November 2022
Revised: 23 December 2022
Accepted: 28 December 2022
Published: 29 December 2022

1. Introduction

Electrical machines play crucial roles in modern societies, e.g., the majority of electricity is generated by electric generators, and a large number of mechanical loads are driven by electric motors. To overcome the problems of fossil fuel depletion, environmental pollution and global warming, it is anticipated that most of the future electrical power will be produced by clean energy sources and most of the mechanical loads will be driven by electric motors. For example, the transportation electrification has recently attracted extensive research interests and the electric motor is among the key technologies. Various electric motors have been developed for driving various electrified vehicles, such as electric bicycles [1], electric cars [2–5], electric buses [6,7], electric trains [8–10], electric ships [11–13] and even electric aircrafts [14,15]. In these vehicles the allowed room and weight are generally quite restricted, so the electric motors should be designed with high power density, but the power loss within certain volume and the associated temperature rise would increase, deteriorating the machine performance and reliability. Therefore, it is crucial to properly consider and predict the power loss and temperature rise in the motor design [16–20].

Magnetic materials, in particular soft ferromagnetic materials, are usually applied as the core of electrical machine and their properties affect the machine performance directly. For electrical machine analysis and design, the core material properties must be available, including the relationship of magnetic flux density (B) versus field strength (H), and associated magnetic power loss, which are usually provided by the material supplier. In general, the magnetic property data are measured on material samples, which usually have magnetic circuits of closed path constructed by stacked lamination steel rings, wound ribbon, solid ring of sintered or bonded powders, or Epstein frame of assembled strips on a frame [21]. In all these types of samples, the B and H are restrained in one orientation.

In electrical machines, however, the tips of B and H vectors are generally two-dimensional (2D) and rotational, and it has been found by various researchers that the magnetic properties under the 2D magnetizations are very different from those under the one-dimensional (1D) alternating flux densities [22–26]. At a low flux density range, the magnetic power loss (core loss) with 2D rotational magnetic fluxes is about twice that with 1D alternating fluxes and goes up with the increase of flux density, but around the saturation point, the core loss may drop greatly if the flux density further increases. This is very different from that the 1D alternating core loss always goes up with the B increase. A number of research works have been performed for modeling the B-H relations under 2D rotation magnetization, such as Stoner–Wohlfarth models [27–29], vectorial Preisach models [30–32], combined models [33,34], E&S model [35,36], and Jiles–Atherton models [37,38]. Some models have also been reported for calculating the 2D rotational core loss in electrical machines [39–43].

In some types of electrical machines, such as claw pole machines and transverse flux machines, the magnetic fields are three-dimensional (3D) and rotational. Naturally, the core material properties under 3D magnetization should be studied and appropriately modeled for the machine design and analysis. This paper targets at an overview about the research works on 3D vectorial magnetic properties of magnetic materials, including the magnetic measurement, mathematical modeling and application prospect.

The rest of the paper is planned as follows. Section 2 introduces a relatively new 3D flux material, soft magnetic composite, which is considered as an ideal core material for designing 3D flux electrical machines. In Section 3, the development of 3D magnetic property testing systems is described. Section 4 discusses the mathematical modeling of the 3D vectorial magnetic properties and how to apply it in the design and analysis of electrical machines. In Section 5, some experimental results of soft magnetic composite (SMC) materials under different 1D, 2D and 3D magnetization patterns are described for implementing and evaluating their application in the electrical machine design and analysis with 3D flux. Finally, Section 6 concludes the paper by discussing possible future research works with the major challenges highlighted.

2. SMC Materials and SMC Electrical Machines

SMC materials possess a number of merits over traditional electrical steel sheets, and hence the materials and their applications in electrical machines have acquired great popularity of research in the past three decades [44–46]. The SMC material basis is the iron powder of high purity and compressibility, and the iron particles are covered with thin insulation, so the material features very high electrical resistivity and very low eddy current loss under varying magnetic fields. The insulated powder articles are pressed into magnetic components with desired shape and dimensions by using the powder metallurgical techniques, so the manufacturing cost can be very low when performing mass production.

The most notable advantage might be the 3D magnetic isotropy caused by the powder nature. This creates the key design benefit as now the electrical machines can be designed with 3D magnetic circuits. In conventional electrical machines with laminated steel sheet cores, the magnetic field path must be within the lamination plane, i.e., 2D. Any magnetic flux component in the third direction, i.e., vertical to the lamination, might induce huge eddy current loss. The SMC material removes this restraint, so that electrical machines can

be designed with great flexibility, and novel configuration with very high-power density becomes possible.

To study the SMC application in electrical machines, a large number of works have been conducted by different scholars. Nearly all kinds of electrical machines have been investigated with the SMC cores, but the most promising types appear to be those with 3D magnetic flux paths, e.g., claw pole machines [47–54] and transverse flux machines [55–60]. As a result, the SMC magnetic properties with 3D magnetic fluxes should be obtained and appropriately modeled for the design and analysis of these 3D flux machines.

3. Measurement of Magnetic Materials under 3D Vectorial Magnetization

3.1. Measuring System of 3D Magnetic Properties

Led by J. Zhu, the University of Technology Sydney (UTS) Magnetic Testing Group developed the world-first 3D magnetic testing system in 2001, as illustrated in Figure 1 [61]. A photo of the 3D magnetic property tester is shown in Figure 2.

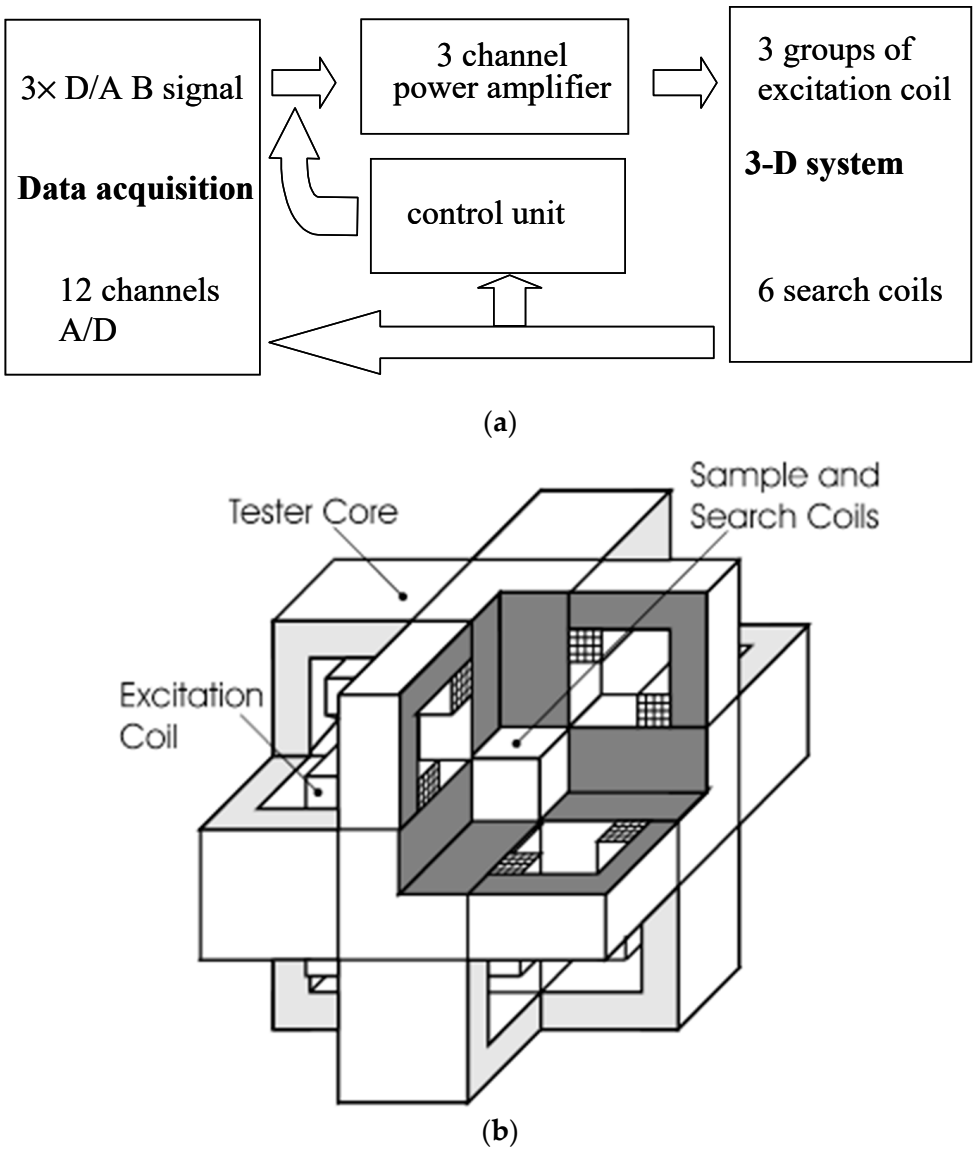

Figure 1. 3D Vectorial Magnetic Property measurement system: (**a**) Block diagram, and (**b**) structure of 3D view.

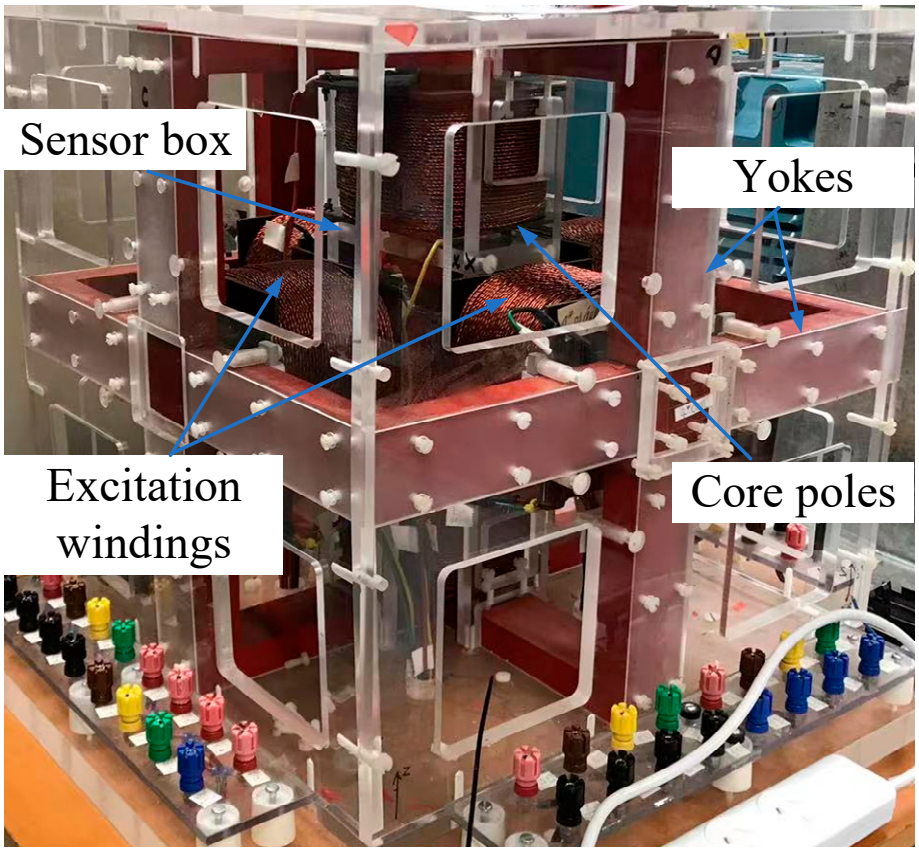

Figure 2. A photo of the 3D vectorial magnetic property measurement system.

The measurement system consists of a 3D magnetic property tester, a computer data acquisition and control system, and a 3-channel power amplifier. Three pairs of excitation windings wound around the six yokes of the tester are used to produce 3D magnetic flux in the material sample, which is located in the tester center. By controlling the magnetic excitations in three axes, i.e., the magnitudes and phase angles of excitation currents, the tester is capable of producing various flux patterns, such as 1D alternating in any specified orientation, 2D circularly or elliptically rotating in a plane tilted for a specified angle from an axis and rotating in a 3D pattern with the loci of the B vector tip forming a specified surface, according to the measurement requirement [62–71].

3.2. Material Sample in the 3D Measurement System

As seen in Figures 1 and 2, a sample of the testing material is put in the middle of the testing system, in which a 3D vectorial magnetization is generated by the currents passing the three excitation coils. In our studies, the sample of cubic shape was manufactured by cutting the preformed SMC material. The size was determined by pre-analysis, e.g., calculating the magnetic field distribution based on 3D finite element analysis. It is important to design the tester and sample capable of generating the requested flux density magnitude and uniformity in the sample with the measurement range of frequency.

3.3. Measurement of 3D Magnetic Field

The magnetic flux density (B) and magnetic field strength (H) sensing coils are employed to measure the B and H components at three axes. As shown in Figure 3, on each surface there are two H coils for measuring the two H components tangential to the surface, and for each axis four coils are connected in series. Three B coils are wrapped around the sample for measuring the B components along three axes.

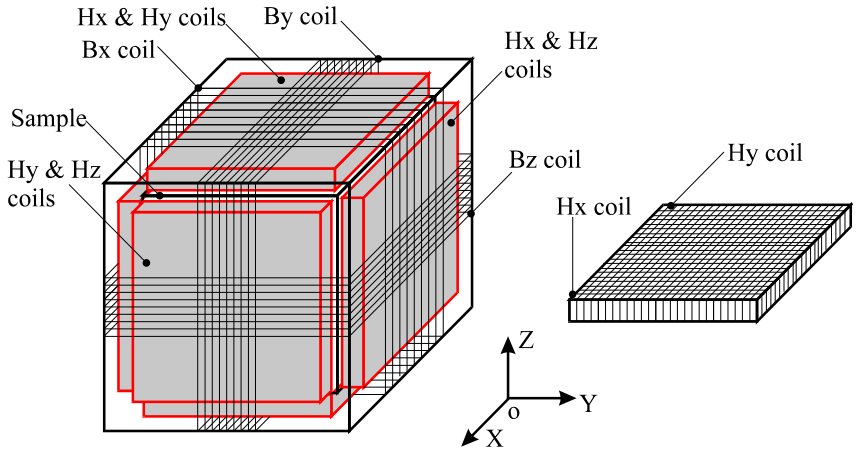

Figure 3. A cubic material sample with **B** and **H** sensing coils.

By measuring the induced electromotive force of the sensing coils, the B and H components along each axis can be worked out by

$$B_i = \frac{1}{K_{B_i}} \int V_{B_i} dt \tag{1}$$

$$H_i = \frac{1}{\mu_0 K_{H_i}} \int V_{H_i} dt \tag{2}$$

where i = x,y,z, K_{Bi} and K_{Hi} are respectively the constants of the B and H coils, and the constants are determined by calibration [72,73].

3.4. Core Loss Testing under 3D Magnetization

When the B and H values have been obtained, the sample core loss P_t in W/kg can be computed according to Poynting's theorem by

$$P_t = \frac{1}{T\rho_m} \int_0^T \boldsymbol{H} \cdot \frac{d\boldsymbol{B}}{dt} dt = \frac{1}{T\rho_m} \int_0^T \left(H_x \frac{dB_x}{dt} + H_y \frac{dB_y}{dt} + H_z \frac{dB_z}{dt} \right) dt \tag{3}$$

where $T = 1/f$ is the excitation period, f is the excitation frequency, and ρ_m is the mass density of the sample material.

4. 3D Vectorial Magnetic Property Modeling and Application

The prediction of B from H or vice versa is necessary for magnetic field analysis of electrical machines. Michelakis et al. proposed a 3D moving vectorial Preisach-type model of hysteresis for magnetic material composed of uniaxial interacting particles [74]. Zhong et al. presented a 3D vector magnetization model based on the 3D Stoner–Wohlfarth element operator, in which a phenomenological mean-field approximation was used to consider the magnetic interactions among particles [75]. Cardelli et al. extended their study on 2D vector hysteresis operator to a 3D case [76]. Li et al. presented a 3D magnetic hysteresis model based on a 3D operator according to the minimum energy principle of a stable magnetization state [77].

The term of magnetic reluctivity or permeability is usually applied to relate the B and H. For 1D alternating magnetic field, the B and H are in the same direction and the constitutive equation can be expressed as

$$\boldsymbol{H} = \nu \boldsymbol{B} \tag{4}$$

The reluctivity ν is a scalar and its value may vary with the change of B, which is called magnetic nonlinearity. For 2D or 3D rotational magnetization, the reluctivity becomes a full 2D or 3D tensor [78–81], and the constitutive equation is

$$H_i = \sum_j \nu_{ij} B_j \tag{5}$$

where ν_{ij} is the reluctivity tensor, $i,j = x,y,z$ in Cartesian coordinates, or r,θ,z in cylindrical coordinates.

The nine elements in the tensor can be obtained by a few measurements under 3D or quasi-3D magnetizations [78]. Then they can be used to solve the 3D magnetic field distribution in electrical machines [82].

5. Implementation and Evaluation of 3D Vectorial Properties of Soft Magnetic Composite Materials in 3D Flux Electrical Machines

Based on the 3D magnetic testing system shown in Figures 1 and 2, some experi-mental results have been obtained with the soft magnetic composite (SMC) samples under various magnetization patterns, e.g., 1D alternating (Figure 4a), 2D circularly rotating (Figure 4b), and 3D spherical flux densities (Figure 4c) at 50 Hz. For 1D case, the relationship of magnetic flux density (B) versus magnetic field strength (H) can be plotted as a series of loops, but the B-H relations under 2D or 3D case become more complex. To work out the corresponding core losses, the Poynting's theorem, given in Equation (3), can be used.

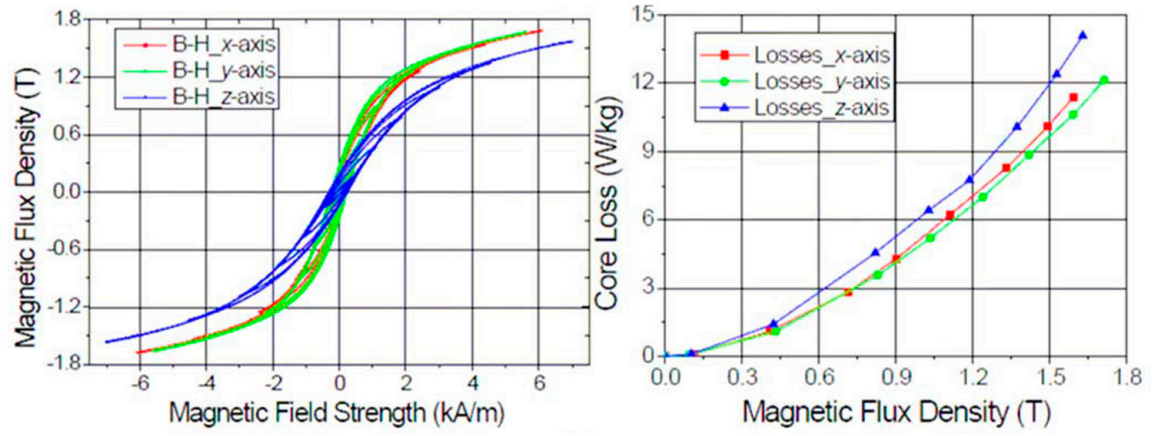

(**a**)

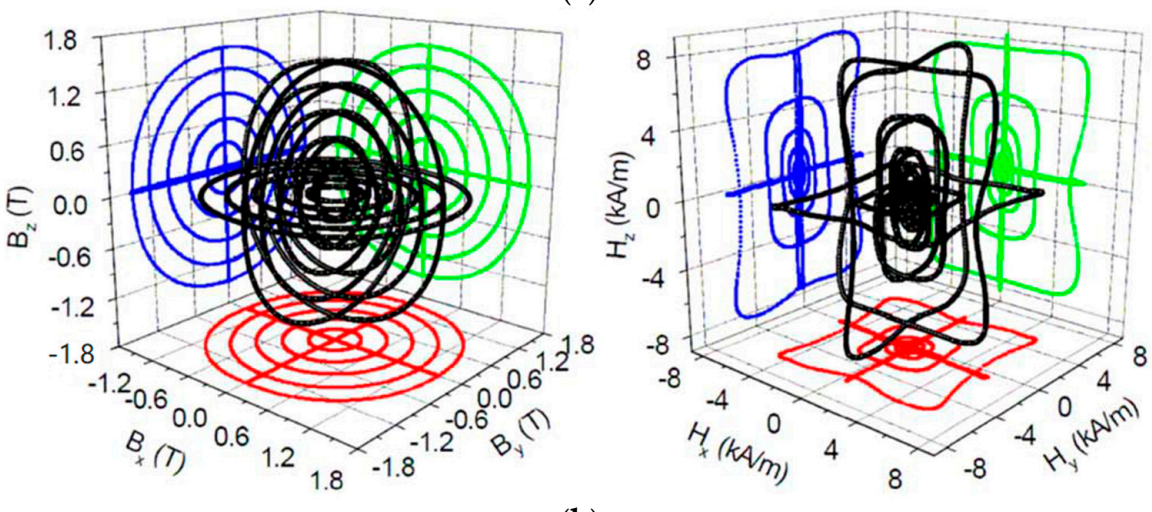

(**b**)

Figure 4. *Cont.*

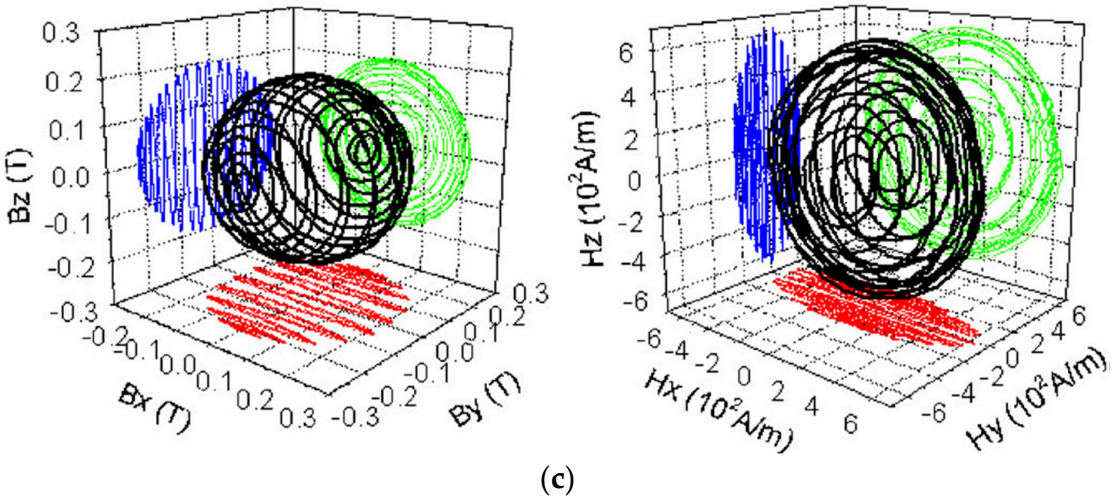

(**c**)

Figure 4. Experimental results of SMC samples at 50 Hz: (**a**) B-H relation and associated core loss under 1D alternating sinusoidal B; (**b**) B-H relation under 2D circularly rotating B; and (**c**) B-H relation under 3D spherical B.

For implementing the measured properties of SMC material samples to the electrical machines with SMC cores, e.g., calculation of core losses, a few SMC machines have been designed, analyzed and prototyped. According to the literature, it might be sufficient to measure the quasi-3D properties, i.e., the 2D circularly rotational magnetic properties on the three orthogonal planes [83]. Based on the 1D alternating and 2D circularly rotating properties, the core losses of SMC electrical machines with 3D flux path have been calculated and the results are found quite close to experiments on motor prototypes, e.g., all within 8% error compared with the measurements [84–87]. By comparison, the calculations using 1D data only would cause a discrepancy of 20–50% from the measurements.

6. Discussions and Challenges

This paper has presented an overview about the study on 3D vectorial magnetic properties of magnetic materials, specifically SMC, for design and analysis of electrical machines with 3D magnetic flux path. In particular, this paper extends greatly the coverage of previous works [65] and discusses the existing challenges and future research trends in this area from a perspective view. As explored above, it would be significant both theoretically and practically to apply 3D vectorial magnetic properties for proper electrical machine design and analysis, but only a couple of groups have conducted research in this area due to the complexities of 3D testing system setup and measurement. The possible future works and challenges are summarized below.

6.1. Standard Masurement and Modeling of 3D Vectorial Magnetic Properties

Although the study on 3D vectorial magnetic properties has already been conducted for two decades, it appears to be still at a very early research stage. For example, the magnetic properties of SMC under true 3D flux density patterns such as a sphere can be measured by using the 3D magnetic testing system, but it is still a pending issue how to apply these properties.

In addition, the sample shape might be an issue. The currently used cubic sample may cause measurement error due to shape factor, but the preferred spherical sample would have difficulties in placing the *B* and *H* sensing coils.

6.2. Infludences of Various Paramaters on Magnetic Properties

The magnetic properties are also influenced by many other parameters, e.g., operational temperature and mechanical stress, which should be properly measured and modeled [88–91]. This is also true for 1D or 2D measurements, but it appears much more

difficult to measure the effects under 3D case, e.g., how to apply 3D compressive or shear forces on the sample which is surrounded by magnetic poles in all three axes. The 3D testing system is generally quite large in size, so a large oven with controllable temperature is needed.

The core loss affects directly the temperature rise as well as mechanical stress, and the temperature and stress also affect the core loss. Therefore, a dynamic modeling considering the two-way effects is desired based on the digital-twin concept [92,93].

Besides the magnetic flux density pattern including waveform, magnitude and frequency, machine operational temperature and mechanical stress, there are many other factors which affect the core loss, such as DC bias of magnetic flux and magnetostriction of the ferromagnetic material. It is very challenging to properly account for all these influencing factors, and in general an appropriate compromise between accuracy and complexity is needed in practice.

Author Contributions: Conceptualization, Y.G., L.L., X.B. and J.Z.; methodology, Y.G., L.L. and J.Z.; software, L.L., H.L. and G.L.; validation, L.L., X.B. and G.L.; formal analysis, H.L. and J.Z.; investigation, Y.G. and L.L.; resources, Y.G., W.Y. and J.Z.; data curation, L.L. and W.Y.; writing—original draft preparation, Y.G. and L.L.; writing—review and editing, Y.G., L.L., X.B., H.L., G.L., W.Y. and J.Z.; visualization, L.L. and H.L.; supervision, Y.G., G.L., W.Y. and J.Z.; project administration, Y.G., H.L. and J.Z.; funding acquisition, Y.G., H.L. and J.Z. All authors have read and agreed to the published version of the manuscript.

Funding: This work was funded by the Australian Research Council under Grants A00104148, LP0454306, DP0667139, and DP180100470.

Data Availability Statement: Not applicable.

Conflicts of Interest: The authors declare no conflict of interest.

References

1. Son, J.-C.; Lim, D.-K. Novel Stator Core of the Permanent Magnet Assisted Synchronous Reluctance Motor for Electric Bicycle Traction Motor Using Grain-Oriented Electrical Steel. In Proceedings of the 2021 24th International Conference on Electrical Machines and Systems (ICEMS), Gyeongju, Republic of Korea, 31 October–3 November 2021; pp. 1215–1218.
2. Zhu, Z.Q.; Howe, D. Electrical Machines and Drives for Electric, Hybrid, and Fuel Cell Vehicles. *Proc. IEEE* **2007**, *95*, 746–765. [CrossRef]
3. Takahashi, T.; Takemoto, M.; Ogasawara, S.; Hino, W.; Takezaki, K. Size and Weight Reduction of an In-Wheel Axial-Gap Motor Using Ferrite Permanent Magnets for Electric Commuter Cars. *IEEE Trans. Ind. Appl.* **2017**, *53*, 3927–3935. [CrossRef]
4. Sun, X.; Shi, Z.; Lei, G.; Guo, Y.; Zhu, J.G. Analysis and Design Optimization of a Permanent Magnet Synchronous Motor for a Campus Patrol Electric Vehicle. *IEEE Trans. Veh. Tech.* **2019**, *68*, 10535–10544. [CrossRef]
5. Bhagubai, P.P.C.; Sarrico, J.G.; Fernandes, J.F.P.; Branco, P.J.C. Design, Multi-Objective Optimization, and Prototyping of a 20 kW 8000 rpm Permanent Magnet Synchronous Motor for a Competition Electric Vehicle. *Energies* **2020**, *13*, 2465. [CrossRef]
6. Ritari, A.; Vepsalainen, J.; Kivekas, K.; Tammi, K.; Laitinen, H. Energy Consumption and Lifecycle Cost Analysis of Electric City Buses with Multispeed Gearboxes. *Energies* **2020**, *13*, 2117. [CrossRef]
7. Xu, Y.; Ai, M.; Xu, Z.; Liu, W.; Wang, Y. Research on Interior Permanent Magnet Synchronous Motor Based on Performance Matching of Electric Bus. *IEEE Trans. Appl. Superconduct.* **2021**, *31*, 5204304. [CrossRef]
8. Guo, Y.; Jin, J.X.; Zhu, J.G.; Lu, H.Y. Design and Analysis of a Prototype Linear Motor Driving System for HTS Maglev Transportation. *IEEE Trans. Appl. Superconduct.* **2007**, *17*, 2087–2090.
9. Torrent, M.; Perat, J.I.; Jimenez, J.A. Permanent Magnet Synchronous Motor with Different Rotor Structure for Traction Motor in High Speed Trains. *Energies* **2018**, *11*, 1549. [CrossRef]
10. Ikeda, R.; Yusya, S.; Kondo, K. Study on Design Method for Increasing Power Density of Induction Motors for Electric Railway Vehicle Traction. In Proceedings of the 2019 IEEE International Electric Machines & Drives Conference (IEMDC), San Diego, CA, USA, 12–15 May 2019; pp. 1545–1550.
11. Yanamoto, T.; Izumi, M.; Yokoyama, M.; Umemoto, K. Electrical Propulsion Motor Development for Commercial Ships in Japan. *Proc. IEEE* **2015**, *103*, 2333–2343. [CrossRef]
12. Li, W.; Ching, T.W.; Chau, K.T.; Lee, C.H.T. A Superconducting Vernier Motor for Electric Ship Propulsion. *IEEE Trans. Appl. Superconduct.* **2018**, *28*, 5201706. [CrossRef]
13. Torrey, D.; Parizh, M.; Bray, J.; Stautner, W.; Tapadia, N.; Xu, M.; Wu, A.; Zierer, J. Superconducting Synchronous Motors for Electric Ship Propulsion. *IEEE Trans. Appl. Superconduct.* **2020**, *30*, 5204708. [CrossRef]

14. Masson, J.; Luongo, C.A. High Power Density Superconducting Motor for All-Electric Aircraft Propulsion. *IEEE Trans. Appl. Superconduct.* **2007**, *15*, 2226–2229. [CrossRef]
15. Tom, L.; Khowja, M.; Vakil, G.; Gerada, C. Commercial Aircraft Electrification—Current State and Future Scope. *Energies* **2021**, *14*, 8381. [CrossRef]
16. Park, H.-J.; Lim, M.-S. Design of High Power Density and High Efficiency Wound-Field Synchronous Motor for Electric Vehicle Traction. *IEEE Access* **2019**, *7*, 46677–46685. [CrossRef]
17. Enokizono, M.; Wakabayashi, D.; Soda, N.; Tsuchida, Y.; Ueno, S.; Oka, M. High Power Density and High Efficiency of High-Speed Motor. In Proceedings of the 2020 International Conference on Electrical Machines (ICEM), Gothenburg, Sweden, 23–26 August 2020; pp. 170–176.
18. Liu, L.; Guo, Y.; Lei, G.; Zhu, J.G. Iron Loss Calculation of High-Speed Permanent Magnet Machines Considering Rotating Magnetic Field and Thermal Effects. *IEEE Trans. Appl. Supercond.* **2021**, *7*, 5205105. [CrossRef]
19. Wu, S.; Zhou, J.; Zhang, X.; Yu, J. Design and Research on High Power Density Motor of Integrated Motor Drive System for Electric Vehicles. *Energies* **2022**, *15*, 3542. [CrossRef]
20. Liu, L.; Ba, X.; Guo, Y.; Lei, G.; Sun, X.; Zhu, J. Improved Iron Loss Prediction Models for Interior PMSMs Considering Coupling Effects of Multiphysics Factors. *IEEE Trans. Transp. Electrif.* **2022**. *early access*. [CrossRef]
21. Fiorillo, F. Measurements of Magnetic Materials. *Metrologia* **2010**, *47*, 114–142. [CrossRef]
22. Brix, W.; Hempel, K.A.; Schroeder, W. Method for the Measurement of Rotational Power Loss and Related Properties in Electrical Steel Sheets. *IEEE Trans. Magn.* **1982**, *18*, 1469–1471. [CrossRef]
23. Enokizono, M.; Shirakawa, G.; Sievert, J. Anomalous Anisotropy and Rotational Magnetic Properties of Amorphous Sheet. *J. Magn. Magn. Mater.* **1992**, *112*, 195–199. [CrossRef]
24. Zhu, J.G.; Ramsden, V.S. Two Dimensional Measurement of Magnetic Field and Core Loss Using a Square Specimen Tester. *IEEE Trans. Magn.* **1993**, *29*, 2995–2997. [CrossRef]
25. Guo, Y.; Zhu, J.G.; Zhong, J.J. Measurement and Modelling of Magnetic Properties of Soft Magnetic Composite Material under 2D Vector Magnetisations. *J. Magn. Magn. Mater.* **2006**, *312*, 14–19. [CrossRef]
26. Xiao, L.; Yu, G.; Zou, J.; Xu, Y.; Wang, M.; Yan, H. A Novel Rotational Single Sheet Tester for Measurement and Modeling of Magnetic Properties of Soft Magnetic Materials under Two-Dimensional Vector Magnetization. In Proceedings of the 2018 21st International Conference on Electrical Machines and Systems (ICEMS), Jeju, Republic of Korea, 7–10 October 2018; pp. 672–679.
27. Stoner, E.C.; Wohlfarth, E.P. A Mechanism of Magnetic Hysteresis in Heterogenous Alloys. *Phil. Trans. Roy. Soc.* **1948**, *240A*, 599–642.
28. Sablik, M.; Jiles, D. A Modified Stoner-Wohlfarth Computational Model for Hysteretic Magnetic Properties in a Ferromagnetic Composite Rod under Torsion. *J. Phys. D: Appl. Phys.* **1999**, *32*, 1971–1983. [CrossRef]
29. Xu, W.; Duan, N.; Wang, S.; Guo, Y.; Zhu, J. A Stress-Dependent Magnetic Hysteresis Model for Soft Magnetic Composite Materials. *IEEE Trans. Appl. Supercond.* **2016**, *26*, 0611305. [CrossRef]
30. Kahler, G.R.; Della Torre, E.; Patel, U.D. Properties of Vector Preisach Models. *IEEE Trans. Magn.* **2005**, *41*, 8–16. [CrossRef]
31. Handgruber, P.; Stermecki, A.; Biro, O.; Gorican, V.; Dlala, E.; Ofner, G. Anisotropic Generalization of Vector Preisach Models for Nonoriented Steels. *IEEE Trans. Magn.* **2015**, *51*, 7300604. [CrossRef]
32. Zhao, X.; Xu, H.; Li, Y.; Zhou, L.; Liu, X.; Zhao, H.; Liu, Y.; Yuan, D. Improved Preisach Model for the Vector Hysteresis Property of Soft Magnetic Composite Materials Based on the Hybrid Technique of SA-NMS. *IEEE Trans. Ind. Appl.* **2021**, *57*, 5517–5526. [CrossRef]
33. Koh, C.S.; Hahn, S.Y.; Park, G.S. Vector Hysteresis Modeling by Combining Stoner-Wohlfarth and Preisach Models. *IEEE Trans. Magn.* **2000**, *36*, 1254–1257.
34. Kahler, G.R.; Della Torre, E.; Cardelli, E. Implementation of the Preisach-Stoner-Wohlfarth Classical Vector Model. *IEEE Trans. Magn.* **2010**, *46*, 21–28. [CrossRef]
35. Soda, N.; Enokizono, M. Improvement of T-Joint Part Constructions in Three-Phase Transformer Core by Using Direct Loss Analysis with E&S Model. *IEEE Trans. Magn.* **2000**, *36*, 1285–1288.
36. Enokizono, M. Loss Evaluation of Induction Motor by Using Magnetic Hysteresis E&S2 Model. *IEEE Trans. Magn.* **2002**, *38*, 2379–2381.
37. Li, W.; Kim, I.H.; Jang, S.M.; Koh, C.S. Hysteresis Modeling for Electrical Steel Sheets Using Improved Vector Jiles-Atherton Hysteresis Model. *IEEE Trans. Magn.* **2011**, *47*, 3821–3824. [CrossRef]
38. Li, J.; Zhang, Y.; Zhang, D.; Ren, Z.; Koh, C.S. Analysis of Rotational Hysteresis Property in a Transformer Core Based on an Inverse Jiles-Atherton Hysteresis Model Coupled with Finite Element Method. In Proceedings of the 2020 23rd International Conference on Electrical Machines and Systems (ICEMS), Hamamatsu, Japan, 24-27 November 2020; pp. 1027–1030.
39. Bertotti, G.; Boglietti, A.; Chiampi, M.; Chiarabaglio, D.; Fiorillo, F.; Lazzari, M. An Improved Estimation of Iron Losses in Rotating Machines. *IEEE Trans. Magn.* **1991**, *27*, 5007–5009. [CrossRef]
40. Zhu, J.G.; Ramsden, V.S. Improved Formulations for Rotational Core Losses in Rotating Electrical Machines. *IEEE Trans. Magn.* **1998**, *34*, 2234–2242.
41. Guo, Y.; Zhu, J.G.; Zhong, J.; Lu, H.Y.; Jin, J.X. Measurement and Modeling of Rotational Core Losses of Soft Magnetic Materials Used in Electrical Machines: A Review. *IEEE Trans. Magn.* **2008**, *44*, 279–291.

42. Sarker, P.C.; Guo, Y.; Lu, H.Y.; Zhu, J.G. Measurement and Modeling of Rotational Core Loss of Fe-Based Amorphous Magnetic Material under 2-D Magnetic Excitation. *IEEE Trans. Magn.* **2021**, *57*, 8402008. [CrossRef]
43. Guo, Y.; Liu, L.; Ba, X.; Lu, H.; Lei, G.; Sarker, P.; Zhu, J. Characterization of Rotational Magnetic Properties of Amorphous Metal Materials for Advanced Electrical Machine Design and Analysis. *Energies* **2022**, *15*, 7798. [CrossRef]
44. Ahmed, N.; Atkinson, G.J. A Review of Soft Magnetic Composite Materials and Applications. In Proceedings of the 2022 International Conference on Electrical Machines (ICEM), Valencia, Spain, 5–8 September 2022; pp. 551–557.
45. Shokrollahi, H.; Janghorban, K. Soft Magnetic Composite Materials (SMCs). *J. Mater. Process. Tech.* **2007**, *189*, 1–12. [CrossRef]
46. Guo, Y.; Zhu, J. Applications of Soft Magnetic Composite Materials in Electrical Machines: A Review. *Aust. J. Electr. Electron. Eng.* **2006**, *3*, 37–46. [CrossRef]
47. Jack, A.G.; Mecrow, B.C.; Maddison, C.P.; Wahab, N.A. Claw Pole Armature Permanent Magnet Machines Exploiting Soft Iron Powder Metallurgy. In Proceedings of the 1997 IEEE International Electric Machines and Drives Conference Record, Milwaukee, WI, USA, 18–21 May 1997; p. MA1/5.1–5.3.
48. Qu, R.; Kliman, G.B.; Carl, R. Split-Phase Claw-Pole Induction Machines with Soft Magnetic Composite Cores. In Proceedings of the Conference Record of the 2004 IEEE Industry Applications Conference, 2004. 39th IAS Annual Meeting, Seattle, WA, USA, 3–7 October 2004; pp. 2514–2519.
49. Guo, Y.; Zhu, J.G.; Watterson, P.A.; Wu, W. Development of a Permanent Magnet Claw Pole Motor with Soft Magnetic Composite Core. *Aust. J. Electr. Electron. Eng.* **2005**, *1*, 21–30. [CrossRef]
50. Huang, Y.; Zhu, J.; Guo, Y.; Lin, Z.; Hu, Q. Design and Analysis of a High-Speed Claw Pole Motor with Soft Magnetic Composite Core. *IEEE Trans. Magn.* **2007**, *43*, 2492–2494. [CrossRef]
51. Guo, Y.; Zhu, J.G.; Dorrell, D.G. Design and Analysis of a Claw Pole Permanent Magnet Motor with Molded SMC Core. *IEEE Trans. Magn.* **2009**, *45*, 4582–4585.
52. Shen, Y.; Zhu, Z.Q.; Chen, J.T.; Deodhar, R.P.; Pride, A. Analytical Modeling of Claw-Pole Stator SPM Brushless Machine Having SMC Stator Core. *IEEE Trans. Magn.* **2013**, *49*, 3830–3833. [CrossRef]
53. Liu, C.; Lu, J.; Wang, Y.; Lei, G.; Zhu, J.; Guo, Y. Design Issues for Claw Pole Machines with Soft Magnetic Composite Cores. *Energies* **2018**, *11*, 1998. [CrossRef]
54. Du, W.; Zhao, S.; Zhang, H.; Zhang, M.; Gao, J. A Novel Claw Pole Motor with Soft Magnetic Composite. *IEEE Trans. Magn.* **2021**, *57*, 8200904. [CrossRef]
55. Blissenbach, R.; Henneberger, G.; Schafer, U.; Hackmann, W. Development of a Transverse Flux Traction Motor in a Direct Drive System. In Proceedings of the ICEM 2000: International Conference on Electrical Machines, Helsinki, Finland, 28–30 August 2000; pp. 1457–1460.
56. Guo, Y.; Zhu, J.G.; Watterson, P.A.; Wu, W. Development of a PM Transverse Flux Motor with Soft Magnetic Composite Core. *IEEE Trans. Energy Convers.* **2006**, *21*, 426–434. [CrossRef]
57. Zhu, J.G.; Guo, Y.G.; Lin, Z.W.; Li, Y.J.; Huang, Y.K. Development of PM Transverse Flux Motors with Soft Magnetic Composite Cores. *IEEE Trans. Magn.* **2011**, *47*, 4376–4383. [CrossRef]
58. Doering, J.; Steinborn, G.; Hofmann, W. Torque, Power, Losses, and Heat Calculation of a Transverse Flux Reluctance Machine with Soft Magnetic Composite Materials and Disk-Shaped Rotor. *IEEE Trans. Ind. Applicat.* **2015**, *51*, 1494–1504. [CrossRef]
59. Liu, C.; Lei, G.; Ma, B.; Wang, Y.; Guo, Y.; Zhu, J. Development of a New Low-Cost 3-D Flux Transverse Flux FSPMM with Soft Magnetic Composite Cores and Ferrite Magnets. *IEEE Trans. Magn.* **2017**, *53*, 1–5. [CrossRef]
60. Rabenstein, L.; Dietz, A.; Parspour, N. Design Concept of a Wound Field Transverse Flux Machine Using Soft Magnetic Composite Claw-Poles. In Proceedings of the 2020 10th International Electric Drives Production Conference (EDPC), Ludwigsburg, Germany, 8–9 December 2020; pp. 1–5.
61. Zhong, J.J.; Zhu, J.G. Electromagnetic Design of a 3D Tester for Magnetic Properties of Soft Magnetic Materials. In Proceedings of the ICEMS'2001. Proceedings of the Fifth International Conference on Electrical Machines and Systems (IEEE Cat. No.01EX501), Shenyang, China, 18–20 August 2001; pp. 392–395.
62. Zhu, J.G.; Zhong, J.J.; Lin, Z.W.; Sievert, J.D. Measurement of Magnetic Properties under 3-D Magnetic Excitations. *IEEE Trans. Magn.* **2003**, *39*, 3429–3431.
63. Guo, Y.; Zhu, J.G.; Lin, Z.W.; Zhong, J.J. Measurement and Modeling of Core Losses of Soft Magnetic Composites under 3-D Magnetic Excitations in Rotating Motors. *IEEE Trans. Magn.* **2005**, *41*, 3925–3927.
64. Zhong, J.J.; Zhu, J.G.; Lin, Z.W.; Guo, Y.G.; Sievert, J.D. Improved Measurement of Magnetic Properties with 3D Magnetic Fluxes. *J. Magn. Magn. Mater.* **2005**, *290–291*, 1567–1570. [CrossRef]
65. Guo, Y.G.; Zhu, J.G.; Lin, Z.W.; Zhong, J.J. 3D Vector Magnetic Properties of Soft Magnetic Composite Material. *J. Magn. Magn. Mater.* **2006**, *302*, 511–516. [CrossRef]
66. Li, Y.; Zhu, J.; Yang, Q.; Lin, Z.; Guo, Y.; Wang, Y. Measurement of Soft Magnetic Composite Material Using an Improved 3-D Tester with Flexible Excitation Coils and Novel Sensing Coils. *IEEE Trans. Magn.* **2010**, *46*, 1971–1974. [CrossRef]
67. Li, Y.; Zhu, J.; Yang, Q.; Lin, Z.; Guo, Y.; Zhang, C. Study on Rotational Hysteresis and Core Loss under three-dimensional magnetization. *IEEE Trans. Magn.* **2011**, *47*, 3520–3523. [CrossRef]
68. Li, Y.; Yang, Q.; Zhu, J.; Guo, Y. Magnetic Properties Measurement of Soft Magnetic Composite Materials over Wide Range of Excitation Frequency. *IEEE Trans. Ind. Applicant.* **2012**, *48*, 88–97. [CrossRef]

69. Yang, Q.; Li, Y.; Zhao, Z.; Zhu, L.; Luo, Y.; Zhu, J. Design of a 3-D Rotational Magnetic Properties Measurement Structure for Soft Magnetic Materials. *IEEE Trans. Appl. Supercond.* **2014**, *24*, 8200804. [CrossRef]
70. Li, J.; Yang, Q.; Li, Y.; Zhang, C.; Qu, B. Measurement and Modeling of 3-D Rotating Anomalous Loss Considering Harmonics and Skin Effect of Soft Magnetic Materials. *IEEE Trans. Magn.* **2017**, *53*, 6100404. [CrossRef]
71. Sun, H.; Li, Y.; Yu, X.; Yue, S.; Yang, M. Research of Harmonic Effects on Core Loss in Soft Magnetic Composite Materials Based on Three-Dimensional Magnetic Test System. In Proceedings of the 2019 22nd International Conference on Electrical Machines and Systems (ICEMS), Harbin, China, 11–14 August 2019; pp. 1–5.
72. Guo, Y.; Zhu, J.; Lin, Z.; Zhong, J.; Lu, H.; Wang, S. Calibration of Sensing Coils of a Three-Dimensional Magnetic Property Tester. *IEEE Trans. Magn.* **2006**, *42*, 3243–3245. [CrossRef]
73. Li, Y.; Yang, Q.; Liu, Y.; Zhao, Z.; Zhang, C.; Li, D. A Novel Combined B-H Sensing Coil in Three-Dimensional Magnetic Properties Testing System. *IEEE Trans. Appl. Supercond.* **2014**, *24*, 9000704. [CrossRef]
74. Michelakis, C.; Samaras, D.; Litsardakis, G. A 3-D Moving Vectorial Preisach-Type Hysteresis Model. *J. Magn. Magn. Mater.* **1999**, *207*, 188–192. [CrossRef]
75. Zhong, J.J.; Zhu, J.G.; Guo, Y.; Lin, Z.W. A 3-D Vector Magnetization Model with International Field. *IEEE Trans. Magn.* **2005**, *41*, 1496–1499. [CrossRef]
76. Cardelli, E.; Torre, E.D.; Faba, A. A General Vector Hysteresis Operator: Extension to the 3-D Case. *IEEE Trans. Magn.* **2010**, *46*, 3990–4000. [CrossRef]
77. Li, D.; Qiao, Z.; Wu, Y.; Li, Z.; Song, Y.; Li, Y. Three-Dimensional Magnetic Hysteresis Modeling Based on Vector Hysteresis Operator. *IEEE Access* **2021**, *9*, 144624–144633. [CrossRef]
78. Guo, Y.; Zhu, J.G.; Lin, Z.W.; Zhong, J.J.; Lu, H.Y.; Wang, S. Determination of 3D Magnetic Reluctivity Tensor of Soft Magnetic Composite Material. *J. Magn. Magn. Mater.* **2007**, *312*, 458–463. [CrossRef]
79. Li, Y.; Yang, Q.; Zhu, J.; Lin, Z.; Guo, Y.; Sun, J. Research of Three-Dimensional Magnetic Reluctivity Tensor Based on Measurement of Magnetic Properties. *IEEE Trans. Appl. Supercond.* **2010**, *20*, 1932–1935.
80. Li, Y.; Zhu, J.; Yang, Q.; Sun, J.; Wang, Y.; Xu, W. Analysis of the 3-D Magnetic Reluctivity Tensor Based on Magnetic Properties Measurement of SMC materials. In Proceedings of the 2010 International Conference on Electrical Machines and Systems, Incheon, Republic of Korea, 10–13 October 2010; pp. 1–6.
81. Li, Y.; Zhao, Z.; Yang, Q.; Wang, Y.; Zhu, J. Tensor Magnetic Reluctivity Properties of Soft Magnetic Composite Materials. In Proceedings of the 2012 Sixth International Conference on Electromagnetic Field Problems and Applications, Dalian, China, 19–21 June 2012; pp. 1–4.
82. Sun, J.; Yang, Q.; Wang, Y.; Yan, W.; Li, Y. A Finite Element Formulation for Tetrahedral Elements Based on Reluctivity Tensor. *IEEE Trans. Appl. Supercond.* **2010**, *20*, 1852–1855.
83. Lin, Z.W.; Zhu, J.G.; Guo, Y.G.; Wang, X.L.; Ding, S.Y. Three-Dimensional Hysteresis of Soft Magnetic Composite. *J. Applied Physics* **2006**, *99*, 08D909. [CrossRef]
84. Guo, Y.; Zhu, J.G.; Zhong, J.J.; Wu, W. Core Losses in Claw Pole Permanent Magnet Machines with Soft Magnetic Composite Stators. *IEEE Trans. Magn.* **2003**, *39*, 3199–3201.
85. Huang, Y.; Zhu, J.; Guo, Y. Thermal Analysis of High-Speed SMC Motor Based on Thermal Network and 3-D FEA with Rotational Core Loss Included. *IEEE Trans. Magn.* **2009**, *45*, 4680–4683. [CrossRef]
86. Guo, Y.; Zhu, J.; Lu, H.; Lin, Z.; Li, Y. Core Loss Calculations for Soft Magnetic Composite Electrical Machines. *IEEE Trans. Magn.* **2012**, *48*, 3112–3115. [CrossRef]
87. Guo, Y.; Zhu, J.; Lu, H.; Li, Y.; Jin, J. Core Loss Computation in a Permanent Magnet Transverse Flux Motor With Rotating Fluxes. *IEEE Trans. Magn.* **2014**, *50*, 6301004. [CrossRef]
88. Lu, H.Y.; Zhu, J.G.; Hui, S.Y.R. Measurement and Modeling of Thermal Effects on Magnetic Hysteresis of Soft Ferrites. *IEEE Trans. Magn.* **2007**, *43*, 3952–3960. [CrossRef]
89. Miyagi, D.; Miki, K.; Nakano, M.; Takahashi, N. Influence of Compressive Stress on Magnetic Properties of Laminated Electrical Steel. *IEEE Trans. Magn.* **2010**, *46*, 318–321. [CrossRef]
90. Ferraris, L.; Franchini, F.; Poskovic, E.; Grande, M.A.; Bidulsky, R. Effect of the Temperature on the Magnetic and Energetic Properties of Soft Magnetic Composite Materials. *Energies* **2021**, *14*, 4400. [CrossRef]
91. Zhang, D.; Shi, K.; Ren, Z.; Jia, M.; Koh, C.-S.; Zhang, Y. Measurement of Stress and Temperature Dependent Vector Magnetic Properties of Electrical Steel Sheet. *IEEE Trans. Ind. Electron.* **2022**, *69*, 980–990. [CrossRef]
92. Mendes, G.; Ferreira, A. Extending the Multiphysics Modelling of Electric Machines in a Digital Twin Concept. In Proceedings of the 2021 11th IEEE International Conference on Intelligent Data Acquisition and Advanced Computing Systems: Technology and Applications (IDAACS), Cracow, Poland, 22–25 September 2021; pp. 689–693.
93. Liu, L.; Guo, Y.; Yin, W.L.; Lei, G.; Zhu, J.G. Design and Optimization Technologies of Permanent Magnet Machines and Drive Systems Based on Digital Twin Model. *Energies* **2022**, *15*, 6186. [CrossRef]